Cellulose Nanocrystals Prepared by Persulfate One-Step Oxidation of Bleached Bagasse Pulp

Chao Du, Mengru Liu, Bingyun Li, Hailong Li,* Qijun Meng, and Huaiyu Zhan

This article describes a novel one-step method to prepare cellulose nanocrystals (CNCs) from bleached bagasse pulp *via* ammonium persulfate (APS) oxidation. The obtained persulfate oxidation cellulose nanocrystals (POCNs) were characterized for their microstructure, crystal properties, and chemical composition. The POCNs were successfully prepared with a total yield of 44.6%. Transmission electron microscopy (TEM) and atomic force microscopy (AFM) measurements indicated that the POCNs had an average length of 150 to 300 nm and an average width of 10 to 30 nm, as well as a rod-like morphology. Fourier transform infrared (FTIR) spectroscopy confirmed the introduction of carboxyl groups on the surface of cellulose. The X-ray diffraction (XRD) spectra proved the existence of cellulose type I, with a highly crystalline nature (79.2%), and thermogravimetric analysis (TGA) showed that the thermal stability decreased.

Keywords: Cellulose nanofibers; Oxidation; Ammonium persulfate; Characterization

*Contact information: State Key Laboratory of Pulp and Paper Engineering, South China University of Technology, Guangzhou 510640, China; *Corresponding author: lihailong1979@gmail.com*

INTRODUCTION

Nanocellulose, a celebrated bio-based nanomaterial, has various outstanding characteristics such as excellent physical strength, high crystallinity, large surface area, unique optical properties, a low coefficient of thermal expansion, and biodegradability (Moon *et al*. 2011; Lee *et al*. 2014). Therefore, nanocellulose has attracted significant interest in both academia and industry, and it is creating a revolution in sustainable biomaterials for various applications, including nanocomposites, food packaging, display substrates, biomedicine, papermaking, and smart materials (Favier *et al*. 1995; De Azeredo 2009; Eichhorn *et al*. 2010; Khalil *et al*. 2012).

Cellulose nanocrystal (CNC) is a type of nanocellulose that consists of rod-like cellulose whiskers with lengths of 100 to 250 nm and widely varied widths of 5 to 70 nm. The methods for preparing and isolating CNCs include acid, enzymes, oxidizers, mechanical means, or a combination of these methods in multiple steps. Acid hydrolysis with, for example, 64% H_2SO_4 at 45 °C for 1 to 4 h, is commonly used to prepare CNCs (Beck-Candanedo *et al*. 2005). When subjected to acid hydrolysis, the amorphous region of cellulose is removed to form highly crystalline nano-scaled whiskers. However, acid-hydrolyzed CNCs usually exhibit a low yield of less than 50% and low aspect ratios that would produce a less efficient reinforcing effect in composites (Dufresne 2012; Isogai 2013). Another type of nanocellulose extracted from lignocellulosic biomass, namely cellulose nanofibrils (CNFs), typically exhibit widths of 5 to 60 nm and lengths ranging from several hundred nanometers to several micrometers (Lu and Hsieh 2010; Klemm *et al.* 2011). Generally, CNF production requires intensive and repeated mechanical

treatments (*e.g*., high-pressure homogenization, grinding, or refining) to achieve the nanofibrillation of native cellulose fibers into nano-sized elements (Siró and Plackett 2010). To greatly reduce the energy consumption of CNF preparation, numerous efforts have combined mechanical treatment with certain enzymatic or chemical pretreatments. Although enzymatic pretreatment requires a lower energy cost and produces a higher yield of CNFs with longer aspect ratios, this technology is limited by enzyme cost and enzymatic accessibility (Zhu *et al*. 2008). Among the chemical pretreatments, oxidation is commonly applied to nanocellulose synthesis. 2,2,6,6-Tetramethylpiperidine-1-oxyl (TEMPO)-mediated oxidation, an approach primarily developed by Isogai and co-workers, is one of the most widely-used methodologies for nanocellulose preparation (Saito *et al*. 2007). During this oxidation process, abundant primary hydroxyls on each cellulose microfibril surface are selectively converted into carboxylate groups under mild and aqueous conditions, which greatly contribute to easy and fast fibrillation because of the strong electrostatic repulsion. This method has numerous merits but also limitations. TEMPO is quite expensive, and the recycling of TEMPO effluents needs future study (Mao *et al*. 2009; Isogai *et al*. 2011). Ammonium persulfate (APS) is a strong oxidizing used industrially as bleaching or cleaning agents. Its use as an oxidant agent to produce cellulose nanocrystals (CNCs) is relatively novel because the free radicals and hydrogen peroxides produced from heating an APS solution are capable of penetrating and breaking down amorphous cellulose to form persulfate oxidation cellulose nanocrystals (POCNs), without any catalysts or mechanical treatments. In recent years, Leung and his co-workers prepared CNCs from cellulose biomass (flax, hemp, triticale, wood pulp, and MCC) by one step, which enable the large-scale production of CNCs (Leung *et al*. 2011).

Sugarcane bagasse is an abundant agro-industrial by-product in China and is an important and excellent fiber source for pulping and papermaking. To investigate the feasibility of preparing CNCs *via* persulfate oxidation, we prepared POCNs from bleach-treated bagasse pulp by one step. The isolated POCNs were fully characterized in terms of morphology, crystallinity, and thermal stability. This project will carry significant benefits in terms of low cost and large-scale production.

EXPERIMENTAL

Chemicals and Materials

Bagasse bleached kraft pulp (88.34% cellulose, 8.94% hemicellulose, and 1.03% lignin) was obtained from Yueyang Paper Co. Ltd., China. Ammonium persulfate ($(NH_4)_2S_2O_8$, APS; > 98% purity] was purchased from the Guangzhou Chemical Reagent Factory (Guangzhou, China). Deionized water was used for all of the experiments.

Methods of CNCs Production

Bleached bagasse pulp (5 g) was added to 500 mL of 1 M APS solution at 1% (w/w) consistency in a 1-L beaker. The mixture was placed in an IKARW20 mixer (IKA Corp., Germany) within a water bath at 65 °C for 8 h at 600 rpm to yield a suspension of POCNs. The suspension was centrifuged at 4000 rpm for 10 min (TDZ5-WS; Cencer Crop., Changsha, China), and 500 mL of deionized water was added to the POCN pellets, followed by mixing and repeated centrifugation until the solution reached pH 7. The product was freeze-dried to yield POCNs power. The oven-drying method was used for yield estimation.

Morphological Characterization

Atomic force microscopy (AFM) measurements were performed in the tapping mode using a Veeco Nanoscope III AFM (Veeco Instruments Inc, New York, USA) at ambient temperature. A drop of diluted aqueous suspension (0.005%) of POCN was dispersed on the surface of a mica plate, allowed to dry under vacuum conditions, and subsequently analyzed. Transmission electron microscopy (TEM; H7650, Hitachi Ltd, Tokyo, Japan) with an acceleration voltage of 80 kV was used to observe the morphology and size of the samples. The POCN suspension (0.01%) was stained with a 3.0% solution of phosphor-tungstic acid for 2 min and dried at room temperature.

Fourier Transformed Infrared (FTIR) Spectroscopy

Fourier transformed infrared spectroscopy was performed using a VerTex70 spectrometer (Bruker Corp., Germany) with freeze-dried samples. Spectra in the range of 400 to 4000 cm^{-1} were obtained at a 4 cm^{-1} resolution.

X-ray Diffraction (XRD) Studies

Diffraction patterns were obtained using a diffractometer (D8 Advance, Bruker AXS, Germany) with Cu Kα radiation (k = 0.154 nm) at 40 kV and 40 mA in the 2θ range of 5° to 60° at a speed of 0.2°/min. The crystallinity index (CrI) was calculated as follows (Segal *et al*. 1959),

$$CrI = ((I_{200} - I_{am})/I_{200}) \times 100 \quad (1)$$

where I_{200} is the diffraction intensity of the crystalline segments at 2θ angle 22° and I_{am} is the diffraction intensity of the amorphous material, which is taken at 2θ angle 18°.

Thermogravimetric Analysis (TGA)

The thermal stability of pulp and freeze-dried POCNs was determined by a thermogravimetric analyzer (Q500/Q50, TA Instruments, USA) under a N_2 atmosphere. The temperature range of 25 °C to 600 °C was maintained at the heating rate of 10 °C/min.

RESULTS AND DISCUSSION

Morphological Analysis

Figure 1a shows a macroscopic image of bleached bagasse pulp and freeze-dried POCN powder with a total yield of 44.6%. In comparison, CNCs obtained from wood pulp and hemp in Leung's work have lower yield (28 to 36%). Figure 1b shows the suspension of pulp and POCNs with a concentration of 0.5 wt%. The pulp was deposited in the bottom of the bottle, while the POCNs were well dispersed in the water, which was white and colloidal in nature. Atomic force microscopy (ATM) and TEM images were used to characterize the surface morphology and dimensional scale of the POCNs. In Fig. 1c and 1d, the diameters of rod-like POCNs ranged from 10 to 30 nm, and the length was determined to be around 150 to 200 nm. In comparison, CNCs produced from bagasse using a combination of bleaching and acid hydrolysis were observed to have rod-like morphology, with an average width of 20 to 40 nm and a particle length of about 170 nm (Pereira *et al*. 2011). The aggregation of POCNs formed larger particles, as evident in the

AFM images; these features were ascribed to strong hydrogen bonding between the fibrils. This aggregation is more obvious when the dispersing medium is removed (Chirayil *et al*. 2014).

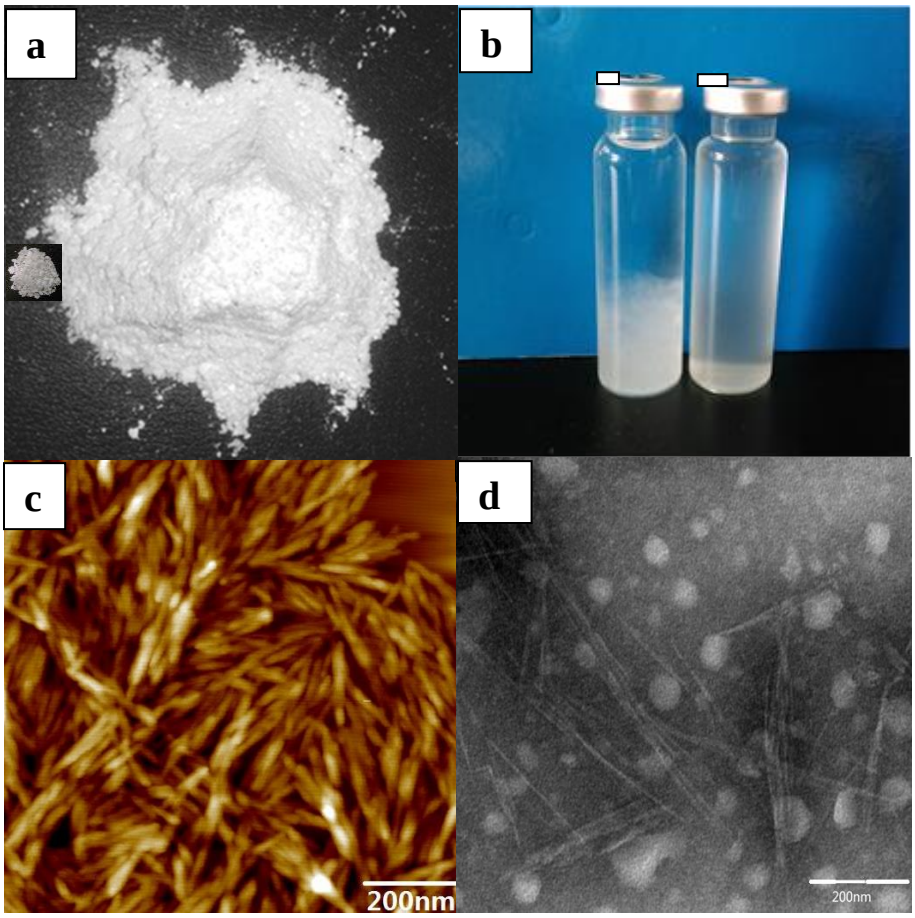

Fig. 1. Photographs of (a) bleached bagasse pulp and POCN powders and (b) aqueous suspensions of bleached bagasse pulp and POCNs; (c) AFM; (d) TEM images of POCNs

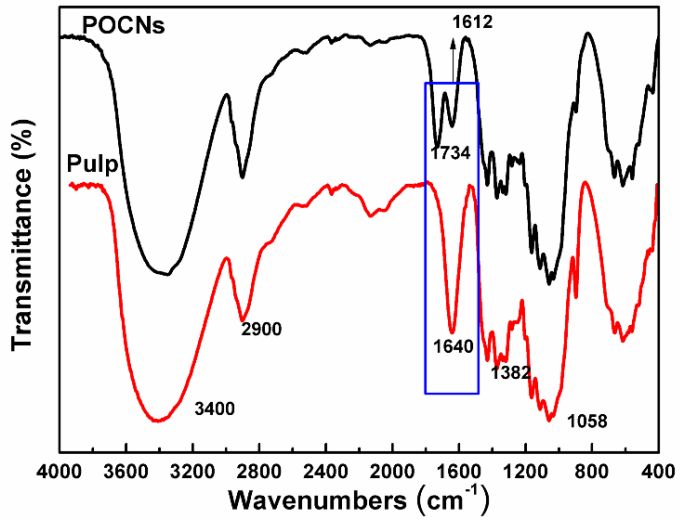

Fig. 2. FTIR spectra of bleached bagasse pulp and POCNs

FTIR Spectroscopy Analysis

The FTIR spectra of pulp and POCNs are shown in Fig. 2. The POCN spectrum displayed a new band at 1734 cm^{-1}, attesting the presence of carboxylic acid groups. The degree of oxidation (DO) of POCNs (DO=1.3) was determined by a conductometric titration method to fall in the range of 0.11 to 0.19, which also was in agreement with Lueng's study (Da Silva Perez *et al*. 2003; Leung *et al*. 2011). The main peaks observed in the two samples included a broad band near 3400 cm^{-1} (O–H stretching vibrations) and a peak at 2900 cm^{-1} (C–H stretching vibrations). The absorption at 1640 cm^{-1} was related to the adsorbed water because of the presence of abundant hydrophilic hydroxide radicals in the cellulose. A peak at 1382 cm^{-1} corresponded to C–H asymmetric deformations. The sharp absorption peaks at around 1058 cm^{-1} were attributed to C–O stretching vibrations (de Souza Lima and Borsali 2004). This result suggested that no other significant chemical reaction occurred during the processes of dissolution and oxidation.

XRD Measurements

X-ray diffraction patterns and the corresponding crystallinity values of pulp and POCNs are shown in Fig. 3. Similar diffraction patterns with four diffraction peaks at the 2θ values of 15.1°, 16.5°, 22.8°, and 34.6° were characteristic of cellulose crystal assignments of the $1\bar{1}0$, 110, 200, and 400 planes, respectively; these patterns resembled typical cellulose-I crystalline structures (Wada *et al*. 2004). In agreement with literature data, X-ray diffraction patterns of POCNs confirmed the integrity of the crystalline structure during the course of APS oxidation (Leung *et al*. 2011). The crystallinity of the POCNs increased from 75.1% to 79.4%, which was ascribed to the progressive removal of cellulose in the amorphous regions. Free radicals are formed when persulfate solution is heated ($S_2O_8^{2-}$ + heat → $2SO_4^{\bullet-}$). In the acidic conditions used in this study, hydrogen peroxide was also formed ($S_2O_8^{2-}$ + $2H_2O$ → $2HSO_4^-$ + H_2O_2). Collectively, the free radicals and H_2O_2 penetrate the amorphous regions to break down amorphous cellulose into POCNs (Hsu *et al*. 2002).

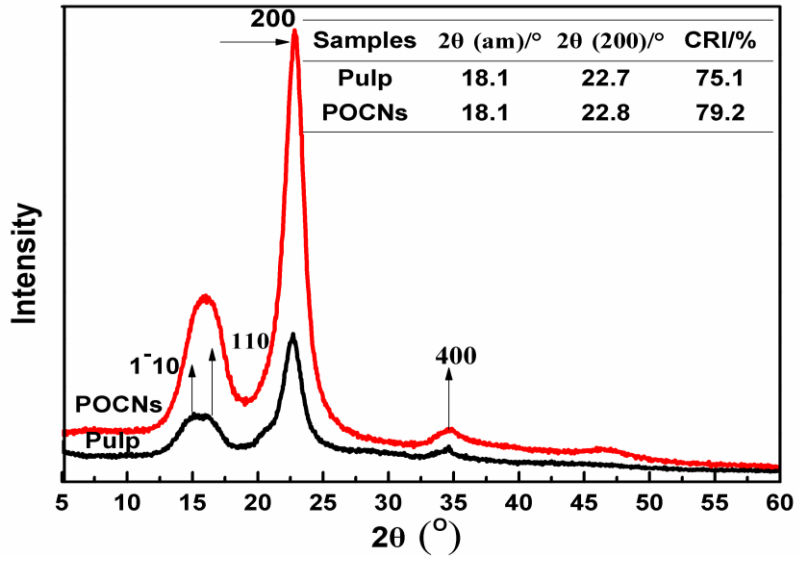

Fig. 3. X-ray diffraction patterns and CRI (inset) for bleached bagasse pulp and POCNs

Thermal Stability of POCNs

Investigating the thermal properties of materials is important for determining their applicability for biocomposite processing at high temperatures. Figure 4 depicts representative thermograms of pulp and POCNs. The pulp displayed the typical degradation profile of cellulose, with an onset temperature of 277 °C. The thermal degradation of POCN began around 224 °C, which was remarkably lower than that of the original pulp. This dramatic decrease was ascribed to the carboxylic groups introduced on the cellulose fiber during APS oxidation (Fukuzumi *et al*. 2008). Furthermore, based on the DTG curves in Fig. 5, the thermal decomposition peaks for the maximum weight loss of the pulp and POCN appeared at 361 °C and 330 °C, respectively. A lowered degradation temperature of POCNs could be attributed to the introduction of carboxylic groups and the microfibrillated cellulose, which increased in the exposure surface area with heating (Stamm 1956; Jiang and Hsieh 2013). An initial small weight loss occurred below 120 °C and was attributed to the water evaporation. The decomposition of POCNs at lower temperatures might indicate faster heat transfer.

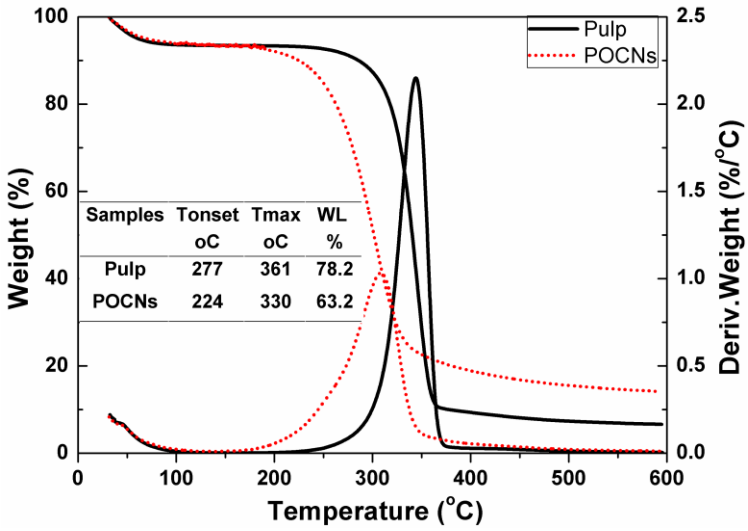

Fig. 4. Thermogravimetric analysis and DTG curves for bleached bagasse pulp and POCNs. The inset table shows the onset temperature (T_{onset}), degradation temperature, T_{max}, and weight loss (WL) of the samples.

CONCLUSIONS

1. Cellulose nanocrystals (CNCs) were successfully isolated from bleached bagasse pulp through persulfate one-step oxidation in the presence of blending action.
2. Different characterization techniques were used to determine properties of cellulose POCNs. AFM and TEM observations showed that the POCNs exhibited a rod-like structure, with widths of 10 to 30 nm and lengths of 150 to 300 nm. FTIR analysis supported the formation of carboxyl groups on the surface of the POCNs, which could be exploited for functionalization reactions with other molecules or reactive groups of polymeric chains. This characteristic is useful for the design of new nanocomposite materials. The POCNs demonstrated crystallinity content increase and lower thermal stability when compared with bagasse pulps.

ACKNOWLEDGMENTS

The authors acknowledge the Science and Technology Planning Project of Guangdong Province, China (No. 2015A020215007), Natural Science Foundation of China (No. 31370585), the Fundamental Research Funds for the Central Universities (No. 2015ZM054 and 2015ZZ048), and the State Key Laboratory of the Pulp and Paper Engineering Program (No. 201434) for sponsoring the research.

REFERENCES CITED

Beck-Candanedo, S., Roman, M., and Gray, D. G. (2005). "Effect of reaction conditions on the properties and behavior of wood cellulose nanocrystal suspensions," *Biomacromolecules* 6(2), 1048-1054. DOI: 10.1021/bm049300p

Chirayil, C. J., Joy, J., Mathew, L., Mozetic, M., Koetz, J., and Thomas, S. (2014). "Isolation and characterization of cellulose nanofibrils from *Helicteres isora* plant," *Industrial Crops and Products* 59, 27-34. DOI: 10.1016/j.indcrop.2014.04.020

Da Silva Perez, D., Montanari, S., and Vignon, M.R. (2003). "TEMPO-mediated oxidation of cellulose III," *Biomacromolecules* 4(5), 1417-1425. DOI: 10.1021/bm034144s

De Azeredo, H. M. (2009). "Nanocomposites for food packaging applications," *Food Research International* 42(9), 1240-1253. DOI: 10.1016/j.foodres.2009.03.019

De Souza Lima, M. M., and Borsali, R. (2004). "Rod-like cellulose microcrystals: structure, properties, and applications," *Macromolecular Rapid Communications*, 25(7), 771-787. DOI: 10.1002/marc.200300268

Dufresne, A. (2012). " Nanocellulose: Potential reinforcement in composites," *Natural polymers: Nanocomposites* (2), 1-32. DOI:10.1039/9781849735315-00001

Eichhorn, S., Dufresne, A., Aranguren, M., Marcovich, N., Capadona, J., Rowan, S., Weder, C., Thielemans, W., Roman, M., and Renneckar, S. (2010). "Review: current international research into cellulose nanofibres and nanocomposites," *Journal of Materials Science*, 45(1), 1-33. DOI: 10.1007/s10853-009-3874-0

Favier, V., Chanzy, H., and Cavaille, J. (1995). "Polymer nanocomposites reinforced by cellulose whiskers," *Macromolecules* 28(18), 6365-6367. DOI: 10.1021/ma00122a053

Fukuzumi, H., Saito, T., Iwata, T., Kumamoto, Y., and Isogai, A. (2008). "Transparent and high gas barrier films of cellulose nanofibers prepared by TEMPO-mediated oxidation," *Biomacromolecules* 10(1), 162-165. DOI: 10.1021/bm801065u

Hsu, Shih-Chang, Trong-Ming Don, and Wen-Yen Chiu. (2002). "Free radical degradation of chitosan with potassium persulfate," *Polymer Degradation and Stability* 75(1), 73-83. DOI: 10.1016/S0141-3910(01)00205-1

Isogai, A. (2013). "Wood nanocelluloses: Fundamentals and applications as new bio-based nanomaterials," *Journal of Wood Science* 59(6), 449-459. DOI: 10.1007/s10086-013-1365-z

Isogai, A., Saito, T., and Fukuzumi, H. (2011). "TEMPO-oxidized cellulose nanofibers," *Nanoscale* 3(1), 71-85. DOI: 10.1039/C0NR00583E

Jiang, F., and Hsieh, Y.-L. (2013). "Chemically and mechanically isolated nanocellulose and their self-assembled structures," *Carbohydrate Polymers* 95(1), 32-40. DOI: 10.1016/j.carbpol.2013.02.022

Khalil, H.A., Bhat, A., and Yusra, A.I. (2012). "Green composites from sustainable cellulose nanofibrils: A review," Carbohydrate Polymers, 87(2), 963-979.DOI: 10.1016/j.carbpol.2011.08.078

Klemm, D., Kramer, F., Moritz, S., Lindström, T., Ankerfors, M., Gray, D., and Dorris, A. (2011). "Nanocelluloses: a new family of nature-based materials," *Angewandte Chemie International Edition* 50(24), 5438-5466. DOI: 10.1002/anie.201001273

Lee, H., Hamid, S., and Zain, S. (2014). "Conversion of lignocellulosic biomass to nanocellulose: structure and chemical process," *The Scientific World Journal*, 1-20. DOI: 10.1155/2014/631013

Leung, A. C. W., Hrapovic, S., Lam, E., Liu, Y., Male, K. B., Mahmoud, K. A., and Luong, J. H. (2011). "Characteristics and properties of carboxylated cellulose nanocrystals prepared from a novel one-step procedure," *Small* 7(3), 302-305. DOI: 10.1002/smll.201001715

Lu, P., and Hsieh, Y.-L. (2010). " Preparation and properties of cellulose nanocrystals: rods, spheres, and network,". *Carbohydrate Polymers* 82(2), 329-336. DOI: 10.1016/j.carbpol.2010.04.073

Mao, L., Ma, P., Law, K., Daneault, C., and Brouillette, F. (2009). "Studies on kinetics and reuse of spent liquor in the TEMPO-mediated selective oxidation of mechanical pulp," *Industrial & Engineering Chemistry Research* 49(1), 113-116. DOI: 10.1021/ie901039r

Moon, R. J., Martini, A., Nairn, J., Simonsen, J., and Youngblood, J. (2011). "Cellulose nanomaterials review: structure, properties and nanocomposites," *Chemical Society Reviews* 40(7), 3941-3994. DOI: 10.1039/C0CS00108B

Pereira, P. H. F., Voorwald, H. C. J., Cioffi, M. O. H., Mullinari, D. R., Da Luz, S. M., and Da Silva, M. L. C. P. (2011). "Sugarcane bagasse pulping and bleaching: Thermal and chemical characterization," *BioResources* 6(3), 2471-2482.

Saito, T., Kimura, S., Nishiyama, Y., and Isogai, A. (2007). "Cellulose nanofibers prepared by TEMPO-mediated oxidation of native cellulose," *Biomacromolecules* 8(8), 2485-2491. DOI: 10.1021/bm0703970

Segal, L., Creely, J., Martin, A., and Conrad, C. (1959). "An empirical method for estimating the degree of crystallinity of native cellulose using the X-ray diffractometer," *Textile Research Journal* 29(10), 786-794. DOI: 10.1177/004051755902901003

Siró, I., and Plackett, D. (2010). "Microfibrillated cellulose and new nanocomposite materials: A review," *Cellulose* 17(3), 459-494. DOI: 10.1007/s10570-010-9405-y

Stamm, A. J. (1956). "Thermal degradation of wood and cellulose," *Industrial & Engineering Chemistry* 48(3), 413-417. DOI: 10.1021/ie51398a022

Wada, M., Heux, L., and Sugiyama, J. (2004). "Polymorphism of cellulose I family: reinvestigation of cellulose IV I," *Biomacromolecules* 5(4), 1385-1391. DOI: 10.1021/bm0345357

Zhu, L., O'Dwyer, J. P., Chang, V. S., Granda, C. B., and Holtzapple, M. T. (2008). "Structural features affecting biomass enzymatic digestibility," *Bioresource Technology* 99(9), 3817-3828. DOI: 10.1016/j.biortech.2007.07.033

Article submitted: December 27, 2015; Peer review completed: February 27, 2016;
Revisions accepted: March 14, 2016. Published: March 17, 2016.
DOI: 10.15376/biores.11.2.4017-4024